

# The elimination of defects in Czochralski grown lithium niobate

T. SUZUKI

*Electronics Materials Laboratory, Sumitomo Metal Mining Co. Ltd, 1-6-1 Suehiro-cho Ohme-shi, Tokyo 198, Japan*

A method is described for growing large  $\text{LiNbO}_3$  single crystals from the melt, completely free of low-angle grain boundaries. This crystalline perfection was achieved by eliminating localized cellular structures, which were introduced by thermal supercooling due to faceted growth. These defects were distributed only near the developed  $(012)_h$  and  $(0\bar{1}\bar{2})_h$  planes when the growth of these planes as facets could be reduced rapidly in the conical part of the boule. Low-angle grain boundaries along the z-axis and polygonization of dislocations were induced by the stresses around the cellular structure. Voids and a corrugated interface have also been observed as a cell-boundary groove trail. The observation of cellular structures indicated that their formation was strongly dependent on growth in the radial direction and the pulled rate. Furthermore, to eliminate these structures, it was found most effective to keep the crystal growth rate,  $G$ , at less than  $10 \text{ mm h}^{-1}$ .

## 1. Introduction

Substructure, mainly low-angle grain boundary or lineage, is a major problem in growing large and good-quality  $\text{LiNbO}_3$  single crystal. Early studies into the crystal growth of  $\text{LiNbO}_3$  and  $\text{LiTaO}_3$  noticed that the presence of low-angle grain boundaries and the orientation of the dislocations determine the final stress distribution in the crystal and the cracking probability [1, 2]. The formation of low-angle grain boundaries can be explained based on the thermally induced internal stress resulting during and after crystallization. This is an important source of dislocations, which, sometimes amalgamate by processes to undergo polygonization, forming low-angle grain boundaries. Similarly, excessive thermal stresses introduce slip or cracking. Crystalline perfection can be improved by employing after-heaters to reduce temperature gradients in the solid [3]. Another interesting mechanism is the morphological instability in undercooling below the equilibrium melting temperature across the interface from the facets. In a given growth system, the supercooling of the facet is related to the radius of curvature of the growth interface, the radius of the facet and the temperature gradient in the solid [4]. This may introduce a cellular structure with dislocations and other crystalline defects, into the crystal.

In the present work, characterization of the large  $\text{LiNbO}_3$  crystal was accomplished by X-ray diffraction topography and chemical etching. Small decanted interfaces, showing a cellular structure, were observed only near  $\{10\bar{2}\}_h$  facets when the diameter of the growing crystal increased rapidly, where a crystal cone is from seed to final diameter. Polygonization of dislocations and low-angle grain boundaries were induced by the stresses around the cellular structure. On the

basis of these observations, the morphological instability applicable to  $\text{LiNbO}_3$  crystals, is discussed.

## 2. Experimental procedure

The crystals were grown using an r.f.-heated Czochralski puller. A platinum crucible was used to contain congruent  $\text{LiNbO}_3$  melts. To improve thermal insulation, the crucible was placed in a ceramic container. The steep temperature gradient directly above the melt was reduced by the use of the after-heater, which was a platinum cylinder placed upon the crucible but separated from it by a zirconia ceramic ring. The purity of the starting materials was at least 99.99%.  $\text{LiNbO}_3$  crystals were pulled along the axis perpendicular to the  $(0\bar{1}4)_h$  plane at a rate of  $2\text{--}10 \text{ mm h}^{-1}$  and the rotational rate was 20 r.p.m. The diameter of the growing crystal was measured under a microscope. Then, the temperature of crucible was adjusted by the r.f. output to generate an angle of the crystal cone in the range from  $90^\circ\text{--}140^\circ$ . The final diameter was about 8 cm. The growing crystals were rapidly pulled from the residual melt for observation of their bottom face. Specimens were prepared by standard techniques with regard to slicing and polishing after making the boules ferroelectrically single domain. The surface normal for the specimen is parallel and perpendicular to the pulling direction.

X-ray topographs were taken by conventional Lang cameras. Direct images of low-angle grain boundaries and cellular structure were obtained in white contrast, where the specimen thickness was  $500 \mu\text{m}$  and  $\text{MoK}_{\alpha 1}$  radiation was used. A scanning electron microscope was helpful to find voids which occurred within the cellular structure. The insulating surfaces were coated

very lightly with a gold film, which was grounded. The negative side of the  $(0\bar{1}4)_h$  plane was etched using a mixed solution of HF and  $\text{HNO}_3$  at  $80^\circ\text{C}$  for 40 min.

### 3. Results and discussion

The bottom face of the  $\text{LiNbO}_3$  crystal cone, as obtained after separation from the residual melt, is shown in Fig. 1. This face, corresponding to the solid-liquid interface, is slightly convex in shape and exhibits two small decanted interfaces. The unstable area averaged about  $2\text{ cm}^2$  in Fig. 2. The bulk contains black fine-line and dot-like defects (Fig. 3). The picture recorded that some stripes and a large triangle present as a ridge on the conical surface, were overlapped [5]. These unstable interfaces were located only under  $(012)_h$  and  $(0\bar{1}2)_h$  planes, and did not appear under the rest of the  $\{10\bar{2}\}_h$  plane. Fig. 4 shows a photograph of a longitudinal cut parallel to the pulling direction of the same crystal as shown in Fig. 1. Developing perturbations can be seen at the decanted interface, showing a cellular structure. The fine-line and dot-like defects are distributed above them. This suggests that they are cell-boundary groove trails. Fig. 5 shows a scanning electron micrograph of a void located

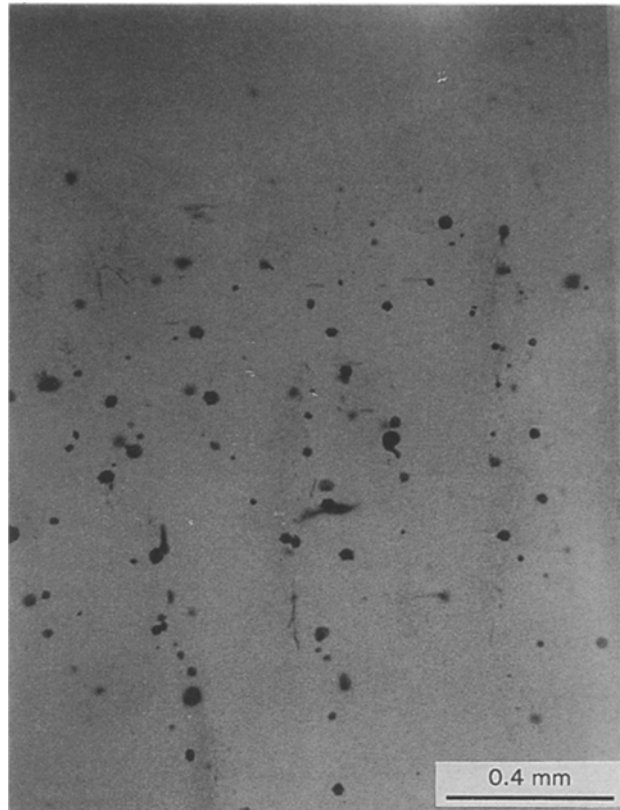


Figure 3 A micrograph of the black fine-line and dot-like defects observed in a cross-section from the crystal cone.

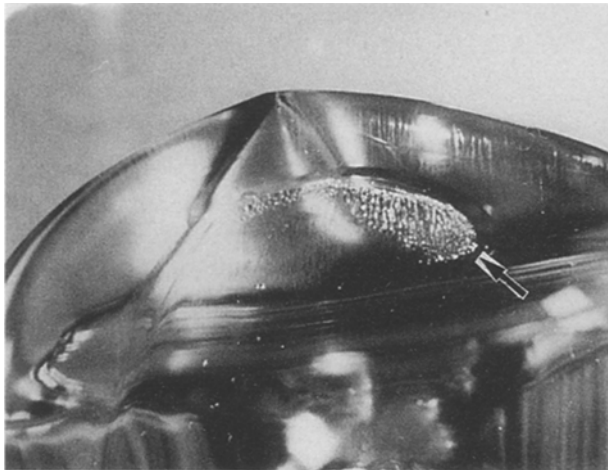


Figure 1 Growth features on the bottom face of a 3 in ( $\sim 7.6\text{ cm}$ ) diameter,  $\text{LiNbO}_3$  single crystal, which was grown at a pulling rate of  $6\text{ mm h}^{-1}$  and generating an angle of  $120^\circ$  in the conical part of the boule. The arrow shows a small decanted interface.

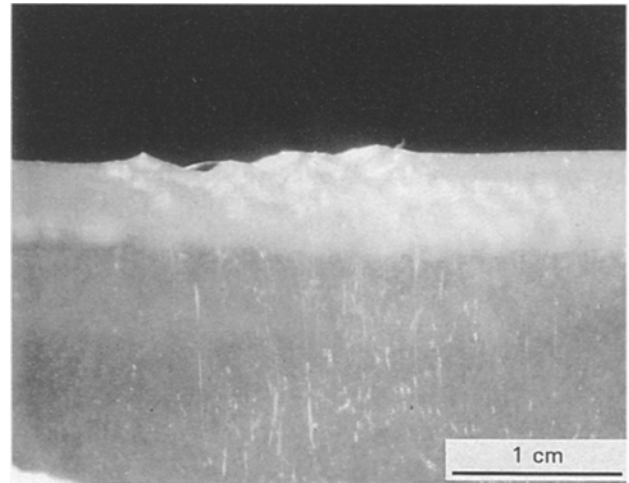


Figure 4 Photograph of the developed perturbations at the decanted interface showing the cellular structure.

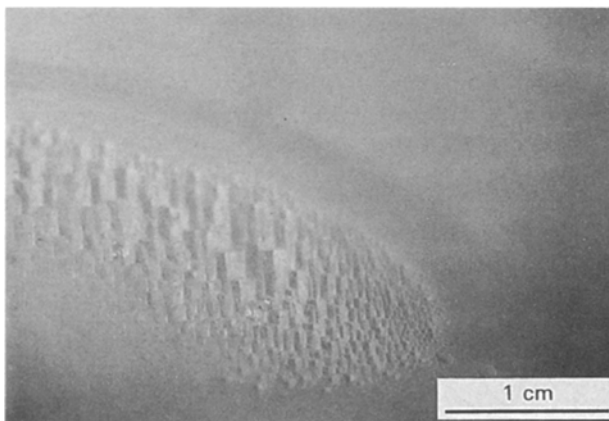


Figure 2 A small decanted interface on the bottom of  $\text{LiNbO}_3$  showing cellular structure.

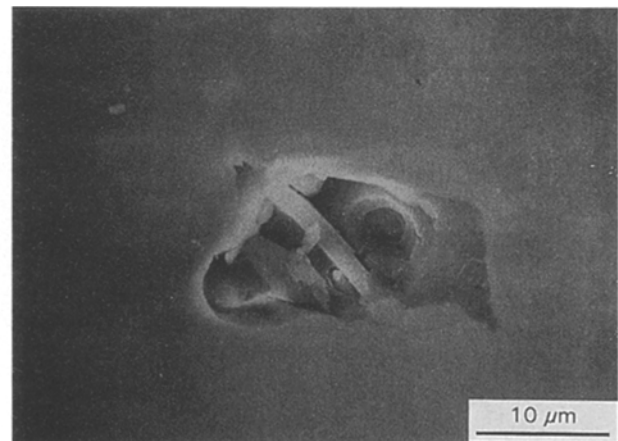


Figure 5 Scanning electron micrograph of a void from the black fine-line and dot-like defects region.

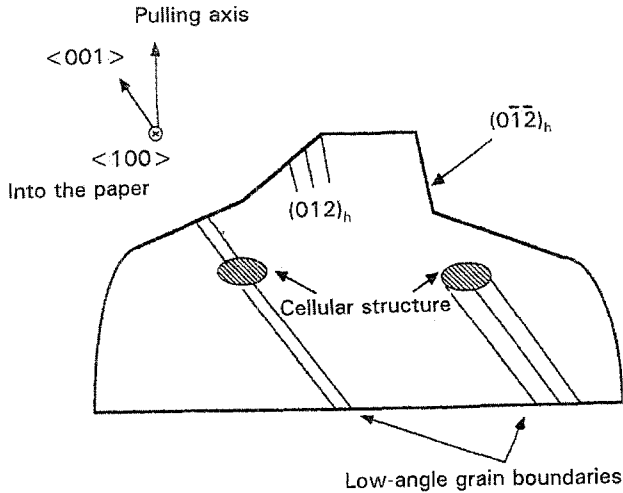
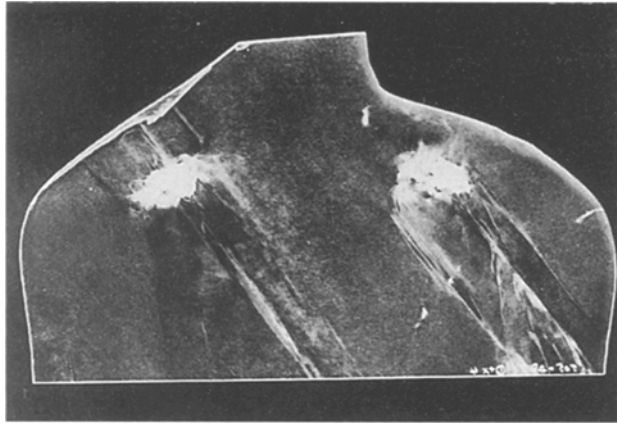


Figure 6 X-ray topograph of a longitudinal cut parallel to the pulling direction.

in the fine-line and dot-like defects due to the cellular structure. The size of the void was about 10–15  $\mu\text{m}$  and was never observed to be over 30  $\mu\text{m}$ . The density was also  $\approx 10^4$  particles  $\text{cm}^{-2}$ . Thus, the fine-line and dot-like defects are attributed to the agglomeration of the voids.

Fig. 6 shows a longitudinal cut parallel to the pulling direction taken as an X-ray topograph. The  $(012)_h$  reflection was used. Marked contrast changes prove that these cellular structures form low-angle grain boundaries along the  $z$ -axis. In faceted growth, crystallization occurs by the formation and lateral spreading of the  $(0\bar{1}\bar{2})_h$  plane. On the contrary, the  $(012)_h$  plane did not appear on the conical surface, because it always grew into the melt. Furthermore, Fig. 7 shows a close-up view of rows of etch pits in the cellular structures. It suggested that polygonization of dislocations is induced by the stresses around them.

The high growth rate,  $G$ , inclusive of growth in the radial direction, causes the cellular structure to occur in the crystal cone, as shown in Fig. 8. The growth rate,  $G$ , is related to the generating angle,  $\theta$ , of the crystal cone by  $G = f \sec(\theta/2)$ , where  $f$  is the pulling rate. In fact, the cellular structures can be eliminated by keeping the growth rate at less than  $G = 10 \text{ mm h}^{-1}$ . It was also found that the large  $\text{LiNbO}_3$  produces no low-angle grain boundaries at a low growth rate.

It is assumed that the growing interface with the developed  $(012)_h$  and  $(0\bar{1}\bar{2})_h$  planes may require

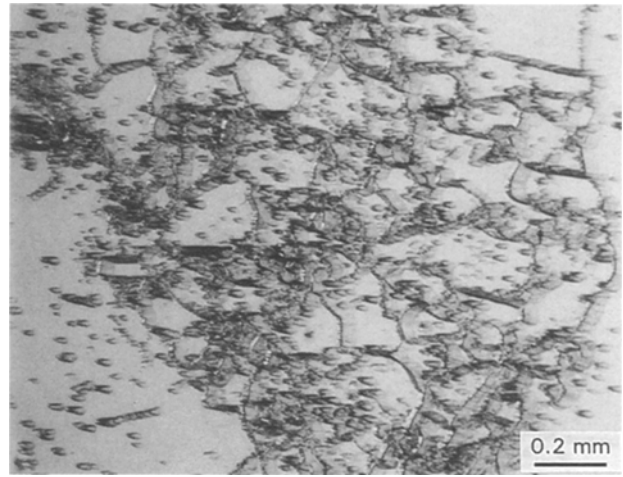


Figure 7 Polygonization of dislocations and low-angle grain boundaries by the cellular structure.

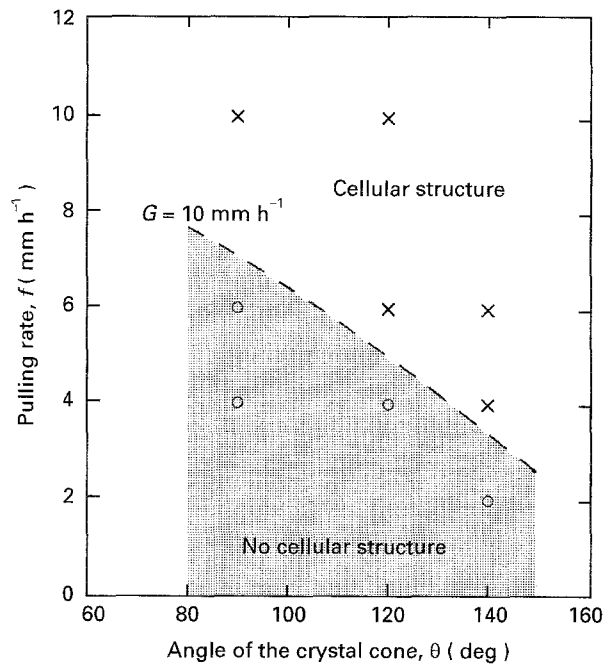


Figure 8 A plot of the pulling rate versus the angle generated in the crystal cone for elimination of cellular structure. Data points are experimental; (o) no cellular structure, and (x) cellular structure. (---)  $G = 10 \text{ mm h}^{-1}$ .

supercooling below its equilibrium melting temperature during growth in the radial direction. However, the growth of these planes as facets will be reduced when the balance between surface tension, viscosity and specific gravity of the melt is broken. This process occurred for crystal diameters over about 20 mm, as shown in Fig. 6. The growth rate,  $G_r$ , for the closing facets will be accelerated from  $G$  of the rest of the interface by thermal supercooling. Also,  $G_r$  is expected to depend only on  $G$  which can determine the faceted area. Therefore, the growing interface becomes unstable as a result of the rapid growth rate,  $G_r$ . The growth instabilities create a cellular structure on the interface.

These unstable interfaces appeared only under  $(012)_h$  and  $(0\bar{1}\bar{2})_h$  planes as a facet, but did not appear under the rest of the  $\{10\bar{2}\}_h$  planes. The angular relation between a plane normal  $n$ , and the melt surface

must be taken into consideration for this difference. On  $(012)_h$  and  $(0\bar{1}\bar{2})_h$ , the angle between  $n$  and the melt surface is  $5.3^\circ$  in the case of pulling along the axis perpendicular to  $(0\bar{1}4)_h$ . These planes will grow rapidly in-plane, once they have nucleated in the interface. As the crystal is continuously pulled from the melt and increases in diameter, the growth planes will hold a small amount of the melt with them. However, the angles of the other planes are too large for the faceted growth to be formed.

Void formation was associated with a rapid increase in the growth rate,  $G_r$ , but voids disappeared when the growth rate  $G_r$  returned to lower values. The formation of voids may be understood as follows. Melt fills the grooves of the cells which are closed by overgrowth. The included melt droplets can create voids during post-crystallization because of volume contraction.

#### 4. Conclusions

It has been shown that one reason for low-angle grain boundaries in large  $\text{LiNbO}_3$  single crystals is cellular structures. These defects were only distributed near the developed  $(012)_h$  and  $(0\bar{1}\bar{2})_h$  planes when the growth of these planes as facets was reduced during growth in the radial direction. Low-angle grain

boundaries along the  $z$ -axis and polygonization of dislocations are induced by the stresses around the cellular structures. Voids and small decanted interfaces have also been observed as a cell-boundary groove trail. These observations have suggested that the morphological instability can be explained based on the faceted growth as a result of the large angle of the crystal cone. The formation of a cellular structure strongly depends on the crystal growth rate,  $G$ , which is related to growth in the radial direction. Thus, to eliminate low-angle grain boundaries due to the cellular structure, it was found most effective to keep the crystal growth rate,  $G$ , at less than  $10 \text{ mm h}^{-1}$ .

#### References

1. C. D. BRANDLE and D. C. MILLER, *J. Cryst. Growth*, **24/25** (1974) 432.
2. S. YASUAMI and T. FUKUDA, *ibid.* **57** (1982) 570.
3. M. C. FLEMINGS, in "Solidification Processing" (McGraw-Hill, New York, 1974) p. 53.
4. J. C. BRICE, *J. Cryst. Growth* **6** (1970) 205.
5. N. NIIZEKI, T. YAMADA and H. TOYODA, *Jpn J. Appl. Phys.* **6** (1967) 318.

*Received 3 March  
and accepted 4 November 1994*